Abstract submitted to SPIE Photonics West 2017, San Francisco, CA. For publisher's version please see: http://dx.doi.org/10.1117/12.2252253

Multi-heterodyne spectroscopy using Fabry-Perot interband cascade lasers for trace gas detection – a feasibility assessment

C. L. Patrick[a], L.A. Sterczewski[ac], J. Westberg[a], W. W. Bewley[b], C. D. Merritt[b], C. L. Canedy[b], C. S. Kim, M. Kim[d], I. Vurgaftman[b], J. R. Meyer[b], and G. Wysocki*[a]

[a]Department of Electrical Engineering, Princeton University, Princeton, New Jersey 08544, USA;
[b]Naval Research Laboratory, Code 5613, Washington, DC 20375, USA;
[c]Faculty of Electronics, Wroclaw University of Science and Technology, Wroclaw 50370, Poland;
[d]Sotera Defense Solutions, Inc., 7230 Lee DeForest Drive, Suite 100, Columbia MD 21046, USA

ABSTRACT

Interband cascade lasers (ICLs) have proven to be efficient semiconductor sources of coherent mid-infrared (mid-IR) radiation. Single mode distributed-feedback (DFB) ICLs are excellent high-resolution spectroscopic sources for targeting important molecular species in the mid-IR fingerprint region, but are limited to a narrow spectral tuning range. Recent developments in multi-heterodyne spectroscopy with multi-mode Fabry-Pérot (FP) lasers have enabled significant progress towards broadband high-resolution spectroscopic sensing applications in the mid-infrared. Here, we characterize the mode structure and tuning properties of multi-mode FP-ICLs for the purpose of evaluating the feasibility of ICL-based multiheterodyne spectroscopy.

Keywords: spectroscopy, interband cascade laser, multiheterodyne

1. INTRODUCTION

The mid-infrared (MIR) portion of the electromagnetic spectrum covers many fundamental rotational-vibrational transitions of molecules of large importance in environmental, industrial, and medical applications[1]. Historically, due to the lack of coherent mid-IR sources, access to the mid-IR spectrum was primarily provided by the Fourier transform infrared (FTIR) spectroscopy technique at the expense of a large footprint, susceptibility to mechanical vibrations, and slow instrument response time. With the development of a novel reliable coherent source of infrared radiation such as early lead-salt lasers[2] and more recently quantum cascade lasers (QCLs)[3] and interband cascade lasers (ICLs)[4-6], all-electronic tunable diode laser absorption spectroscopic (TDLAS) techniques gained popularity in the MIR[7]. Initially, these systems were mainly based on single mode lasers in the distributed feedback (DFB) configuration. Although these lasers enabled a spectral resolution down to the MHz together with fast acquisition rates, their tuning capabilities were limited to single cm^{-1}. This problem was overcome by employing an external cavity configuration enabling broadband acquisition with up to two orders of magnitude increase in spectral coverage. However, these systems were not free from opto-mechanical elements and hence are sensitive to mechanical vibrations, which limits their utility to well-controlled laboratory based systems.

Lately, much attention has been devoted to Fabry-Pérot (FP) devices and their application to spectroscopy. An important discovery has been made in case of FP-QCLs, since they have been shown to emit stable optical frequency combs (OFC) generated intrinsically within the laser medium due to a sufficiently low intracavity dispersion[8]. Through proper dispersion engineering, FP-QCLs have shown reliable OFC generation over the entire tuning range[9]. Consequently, a dual comb spectroscopic technique that utilizes two optical frequency combs with slightly different repetition rates heterodyned on a photodetector to down-convert the spectroscopic information could be conveniently realized with an unprecedented scale of miniaturization[10]. The main advantages of this multi-heterodyne spectroscopy (MHS) technique are fast acquisition rates, broad spectral coverage, high resolution, and solid state operation[11]. This was further extended by the demonstration of its compatibility with modulation techniques, such as wavelength modulation (WMS)[12], swept absorption, and swept dispersion spectroscopy[13].

Interband cascade lasers (ICL) provide an alternative to the inter-subband architecture of QCLs[4-5] with high efficiencies (up to 18% wall-plug for cw at room temperature), lower bias voltages, and lower threshold currents that can be comparable to those of mature near-IR diode lasers. Consequently, they are very suitable for battery-operated portable spectroscopic

*gwysocki@princeton.edu;

systems that demand energy-efficient operation. ICLs have been demonstrated to operate between 3 µm and up to 7 µm, with the best performance typically within the 3-4 µm range where many environmentally important trace gas species have strong absorption cross sections (methane, carbon dioxide, carbon monoxide, etc.). The best ICL devices with low threshold current densities and low bias voltages provide continuous-wave (CW) threshold drive powers as low as tens of mW even at room-temperature[6]. Such capability makes them particularly suitable for hand-portable units or other field-deployable instruments with power consumption constraints. Therefore, it has become important to study the parameters of FP-ICLs and their suitability to perform MHS.

In this work, we have characterized the operation of an FP-ICL at ~3.25 µm for trace gas sensing in a MHS configuration. The device develops a broadband structure of modes at currents as low as 50 mA. We study the injection current and temperature tuning characteristics simultaneously in the optical and radio-frequency (RF) domains to determine the optimal regions for low-noise, comb-like operation.

2. EXPERIMENTAL RESULTS

2.1 ICL characterization

Light-current-voltage characteristics

Two ICLs have been characterized for application in a MHS setup. The collimated ICLs were mounted in thermoelectrically-cooled laser housings (LDM-487201) and biased using low-noise QCL500 drivers supplied from an isolated linear power supply. The ICLs emitted an optical power of ~30 mW while consuming ~530 mW of electric power. Figure 1 displays the light-current-voltage (LIV) curves acquired for one of the two lasers operated between 10 and 20°C. The maximum optical power decreases by 11% in this temperature range, and consequently the wall-plug efficiency decreases proportionately.

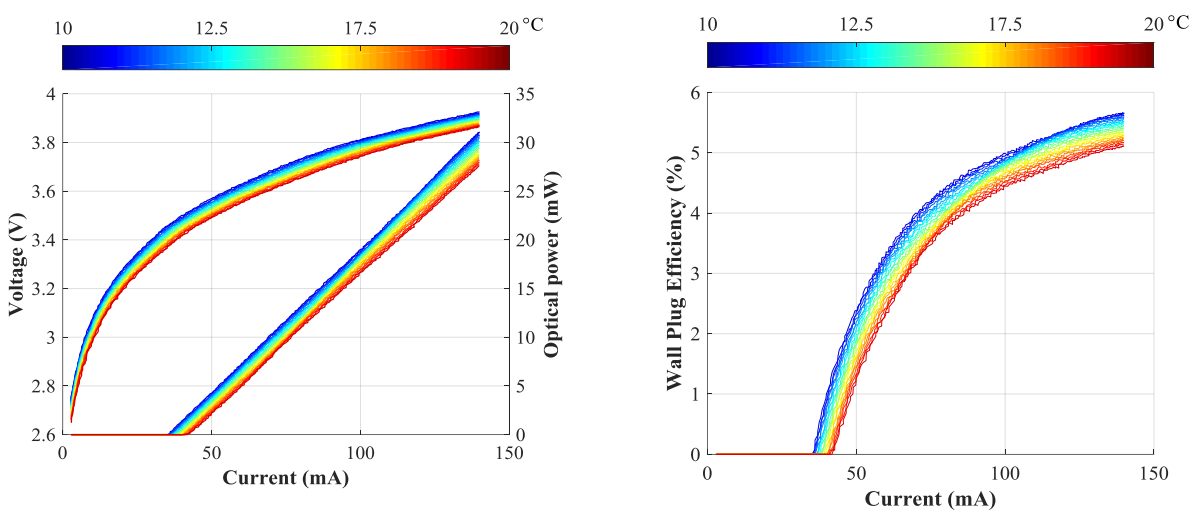

(a) (b)

Figure 1. (a) LIV curve and (b) wall-plug efficiency of an ICL at temperatures varying from 10 to 20°C.

FTIR spectrum coupled with RF noise measurements

The series of optical spectra measured by an FTIR (Nicolet 8700) shows the evolution of modes as a function of injection current at a constant temperature, and as a function of temperature at a constant current in Figures 2 and 3, respectively. Figures 2 and 3 also show simultaneous measurements of the RF laser intensity noise. Figure 4 shows a single FTIR spectrum at 20°C and 137 mA (indicated in Fig. 2a by the red dashed line). In Figure 2 (constant temperature, variable current mode) it can be seen that the laser develops modes in groups with characteristic gaps in the spectrum. At around 90 mA another group of modes starts lasing that causes an increase in broadband RF noise. The development of a third mode group above 112 mA causes the broadband RF noise to further intensify.

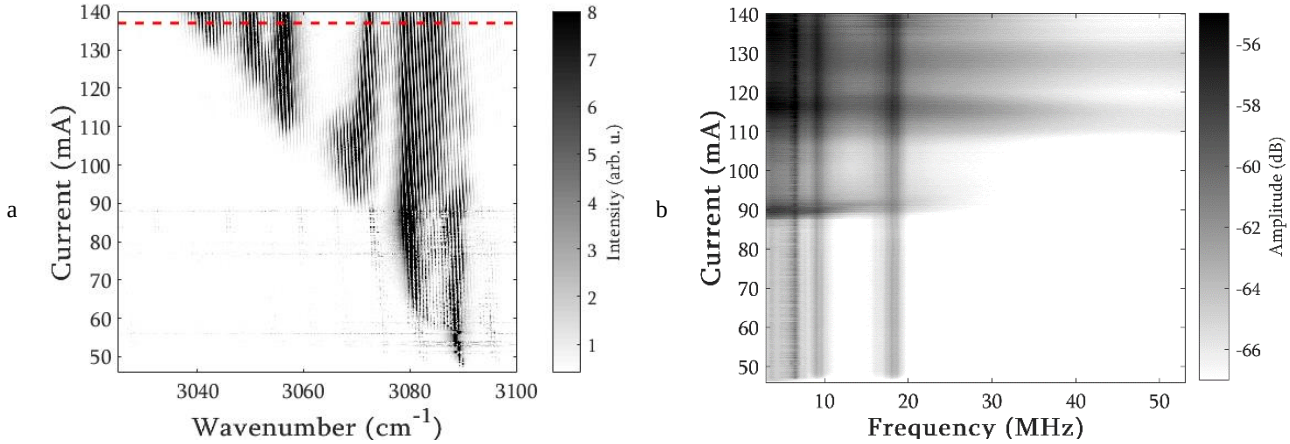

Figure 2. (a) shows the optical spectrum of an ICL and (b) shows the RF noise spectrum as a function of current measured at 20°C.

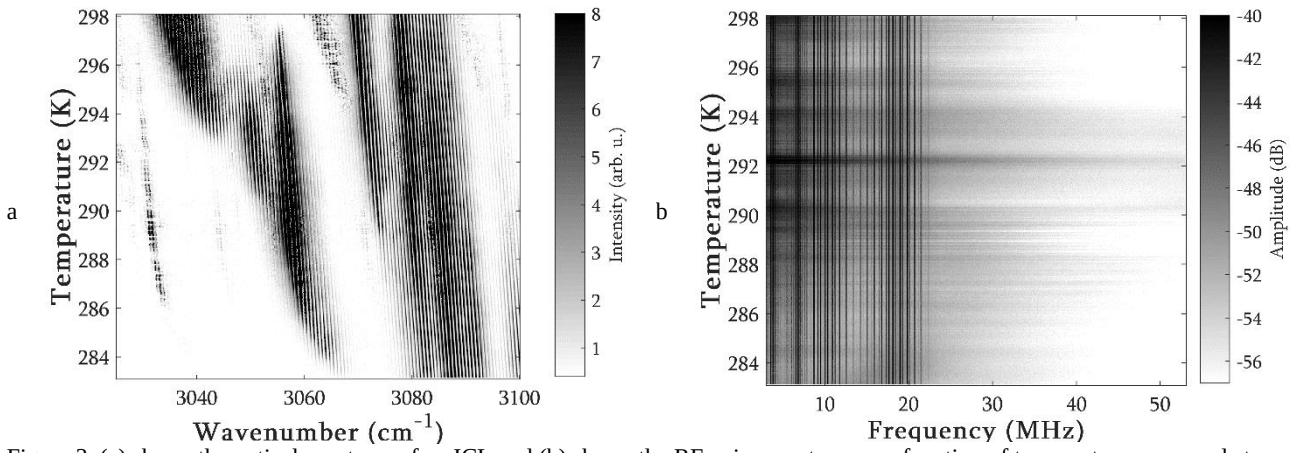

Figure 3. (a) shows the optical spectrum of an ICL and (b) shows the RF noise spectrum as a function of temperature measured at 130 mA.

The temperature tuning data (Figure 3) reveal that the gaps in the spectrum are thermally tunable to some extent. Also, at higher temperatures a group of modes centered around 3060 cm^{-1} disappears and is replaced by another at 3040 cm^{-1}, which reduces the RF noise at around 294 K. Based on these measurements, we have identified a range of temperatures and currents that provide a broad spectrum with low RF noise, which is suitable for MHS. The optimum current range of 90-110 mA is delineated by the increased RF noise above 110 mA and by the small number of available FP modes below 90 mA. By performing this characterization procedure for two lasers with similar free spectral range, optimum operating regimes for MHS were clearly identified.

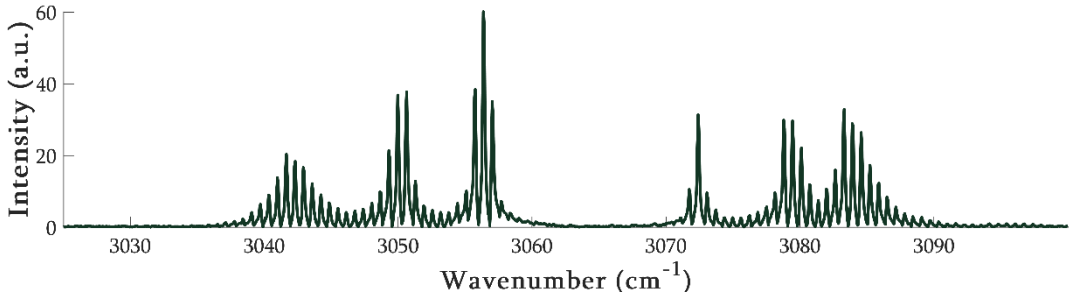

Figure 4. Optical spectrum of an ICL at 20°C and 137 mA, corresponding to the dashed red line in Figure 2.

Near-threshold spectrum

Figure 5 shows that the ICL under test exhibits an interesting behavior just above the lasing threshold. While it initially operates in a single mode, as expected, increasing the current gives rise to symmetrically-distributed satellites containing small sub-groups of modes that are spaced by approximately 25 cm^{-1}. The symmetric distribution of the satellite groups is coupled with broadband coverage (>175 cm^{-1}). This regime corresponds also to a very low intensity of the RF noise (not shown). Such behavior has been seen previously[14], since it resembles the formation of sub-combs in a microresonator[15]. At approximately 48 mA, this regime transforms into the regular multi-mode operation of the ICL with much narrower spectral coverage.

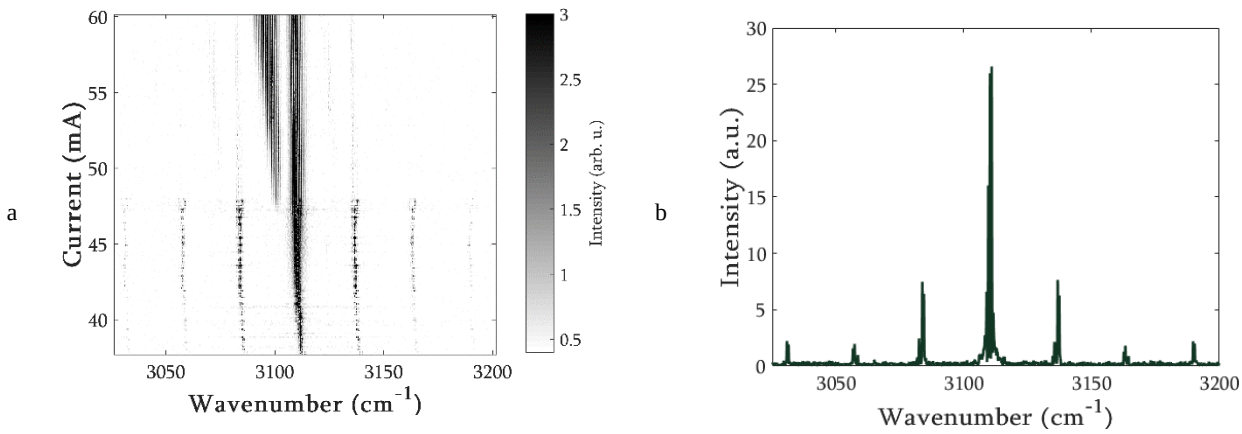

Figure 5. (a) Optical spectrum of an ICL near current threshold at 12°C. A change in output behavior is clearly seen at 48 mA. (b) optical spectrum at ~46 mA showing the symmetric distribution of sub-groups of optical modes that collectively span more than 175 cm^{-1}.

2.2 Frequency Tuning

As shown in the previous sections, the optical modes tune considerably as a function of current and temperature. The tuning relationship is nominally linear with the following rates for the optical offset: current tuning of 40 cm^{-1}/A and temperature tuning of 0.33 cm^{-1}/K.

However, the linearity assumption does not accurately describe the evolution of the individual ICL modes. As may be seem from the closer look at the intermittent behavior in Figure 6a, the tuning trajectory visibly changes around 90 mA. To analyze this phenomenon, the FTIR spectrum is interpolated to track the center position of the individual modes. Next, a second order polynomial is fitted to the data (R^2>0.99 for all modes), as illustrated in Figure 6b for one of the modes together with a residual fit in Figure 6c that reveals a finer structure.

By comparing Figure 2a with the corresponding fit coefficients for different modes (Figure 6d), one can see that the region 3080-3090 cm^{-1} has the lowest variation of the tuning between neighboring modes. Parts of the spectrum below 3080 cm^{-1} possess large differences between the neighbors with enormously high nonlinearities. Notably, the highly scattered fit coefficients indicate regions of the spectrum that contribute increased RF noise. Consequently, the high-wavenumber region with slowly-varying fit coefficients and low RF noise is the most suitable for MHS.

To further analyze the mode-by-mode tuning behavior in the MHS-suitable range, the residuals from the fit are plotted in Figure 6e. It clearly displays significant fluctuations below 90 mA, with modes near the ends exhibiting the greatest shift in frequency. The appearance in Figure 6e of mirrored symmetry about the 3085.7 cm^{-1} mode suggests some frequency pulling that may be related to the two dominant groups of modes observed on both sides of this frequency. Similar frequency tuning analysis has been performed with QCLs[16], which demonstrate similar behavior and performance.

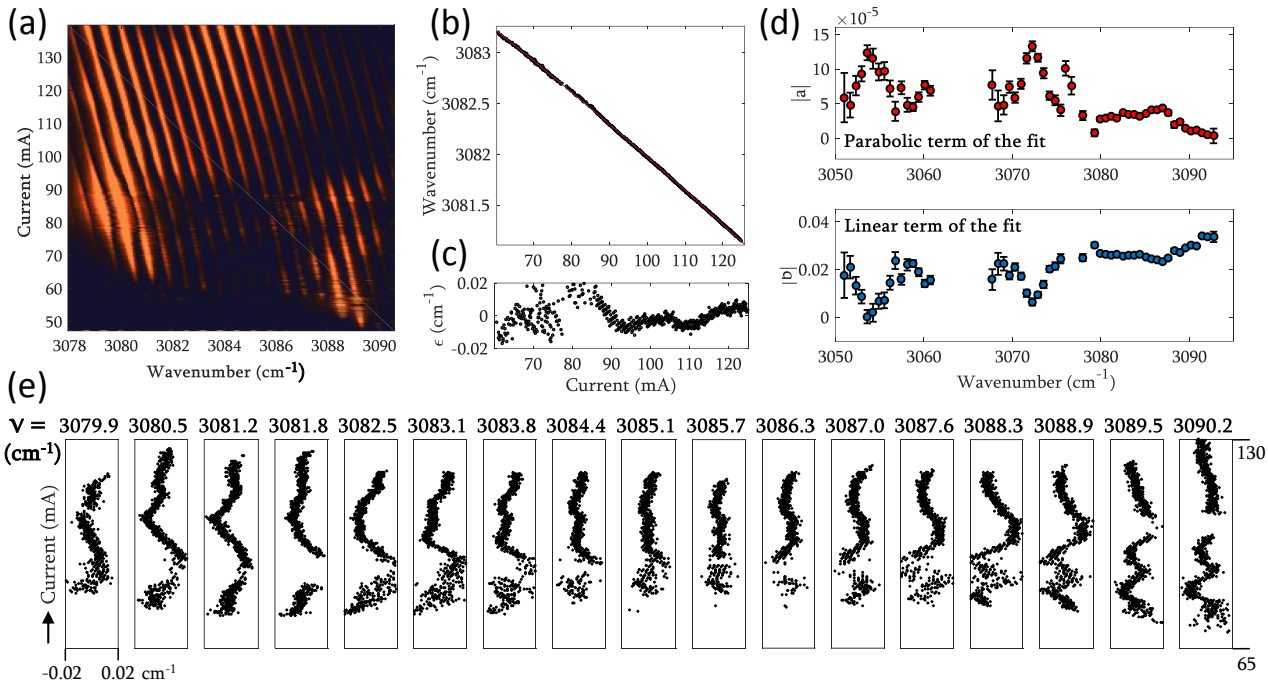

Figure 6. (a) shows a close-up the optical modes to highlight to change in operation near 90mA. (b) Parabolic fit of optical mode and (c) the residuals of the fit. (d) The fit coefficients for each mode. (e) Residuals for each fit of each mode between 3080-3090 cm^{-1}.

2.3 Multiheterodyne Signals

Despite the increased noise and nonlinear tuning characteristics of the laser, the ICL is comparable in performance to the QCL and is suitable for MHS. Two ICLs from the same batch, but cleaved to slightly different cavity lengths to provide slightly different free spectral ranges (FSR) of 0.640 and 0.643 cm^{-1} ($\Delta FSR \approx 96$ MHz), were biased in the low phase noise regime and optically heterodyned at a high-bandwidth photodetector (VIGO PV-4TE-10.6). Figure 10 illustrates a simple MHS experimental setup. Due to the slight difference in FSR, the optical modes from the two lasers produce a series of beat notes in the RF domain separated by ΔFSR (see Fig. 11). This allows the spectroscopic information to be down-converted from the optical domain to RF frequencies. At the optimal current and temperature, up to 20 optical modes are present within the bandwidth of the photodetector, each with sub-milliwatt light intensity.

When taking a measurement, the RF spectrum is measured from both detectors (Vigo PV-4TE-10.6) by a 20 GHz oscilloscope (LeCroy WavePro 735Zi). 40 dB low-noise amplifiers (Pasternack PE15A1012) are used to boost the signal fed into the oscilloscope. The RF beat notes are positioned by varying the current so that the negative-frequency beat notes are folded into the positive part of the RF spectrum[17]. This overlapping allows more beat notes to be packed into the bandwidth of the detector. The observed RF spectrum in Fig. 11 confirms the effectiveness of ICLs for MHS.

3. DISCUSSION AND CONCLUSION

In conclusion, ICLs are promising multi-mode MIR light sources that exhibit low phase noise behavior in some operating regimes, so as to allow broadband measurement with MHS. Frequency tuning by current and temperature is possible in selected spectral regions, 0-25°C and 90-110 mA. In comparison to QCLs, ICLs possess lower threshold current and voltage, as well as high wall-plug efficiency, and display similar spectral mode formation at a small cost of larger RF noise. The measured RF beat note spectrum indicates that MHS with FP-ICLs is feasible. In the next stage of this work, we plan to improve the ICL frequency drift and linewidth by implementing a frequency-discriminator-based PID control loop, similar to that shown in one of our previous works on QCLs[8]. Moreover, coherent averaging techniques and/or computational post-processing will be applied to achieve better spectroscopic assessment and higher signal-to-noise ratio[18].

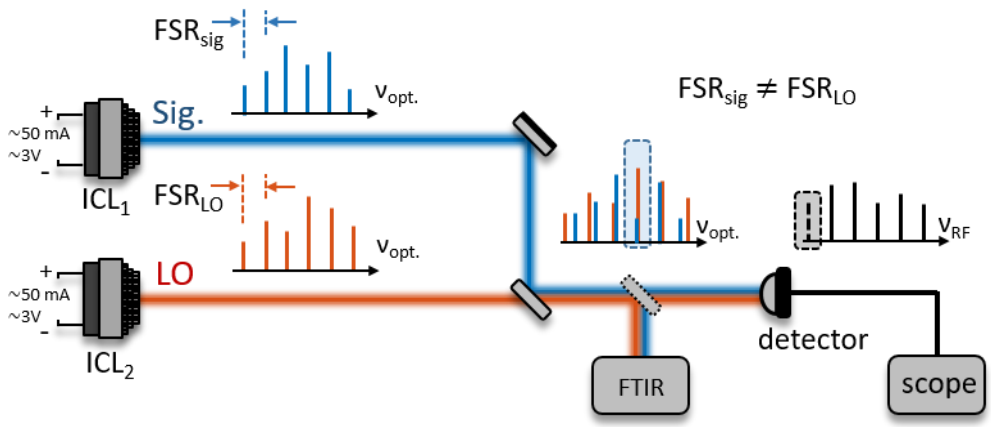

Figure 10. Multiheterodyne experimental setup.

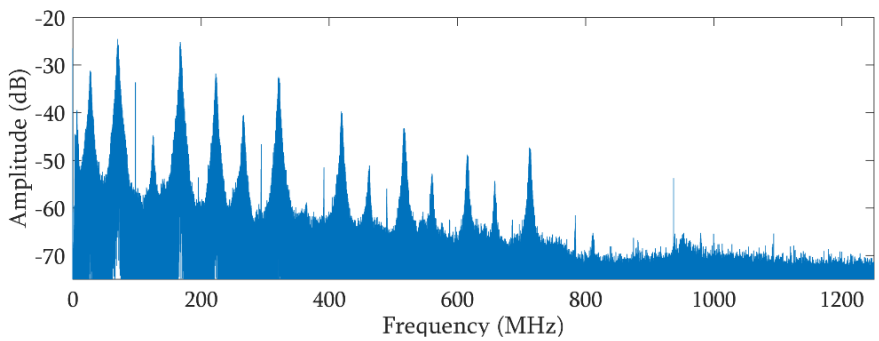

Figure 11. Raw multiheterodyne RF beat note spectrum. Beat note linewidth is ~1MHz and the SNR is ~20dB.

Acknowledgements: This research was founded by the DARPA SCOUT program (W31P4Q161001); and NSF ERC MIRTHE (EEC-0540832).

REFERENCES

[1] Coddington, I., Newbury, N. and Swann, W., "Dual-comb spectroscopy," Optica 3, 414 (2016).
[2] Mirov, S., Fedorov, V., Moskalev, I., Mirov, M., and Martyshkin, D., "Frontiers of mid-infrared lasers based on transition metal doped II–VI semiconductors," Journal of Luminescence, 133, 268-275 (2013).
[3] Faist, J., Capasso, F., Sivco, D. L., Sirtori, C., Hutchinson, A. L. and Cho, A. Y., "Quantum Cascade Laser", Science 264(5158), 553-556 (1994).
[4] Yang, R. Q., "Infrared laser based on intersubband transitions in quantum wells," Superlattices Microstruct. 17, 77–83 (1995).
[5] Vurgaftman, I. et al., "Interband cascade lasers," J. Phys. Appl. Phys. 48, 123001 (2015).
[6] Vurgaftman, I. et al., "Rebalancing of internally generated carriers for mid-infrared interband cascade lasers with very low power consumption," Nat. Commun. 2, 585 (2011).
[7] Tittel, F., Bakhirkin, Y., Kosterev, A., Kosterev, A. and Wysocki, G., "Recent Advances in Trace Gas Detection Using Quantum and Interband Cascade Lasers," The Review of Laser Engineering 34, 275-282 (2006).
[8] Hugi A., Villares G., Blaser S., Liu H. C., and Faist J., "Mid-infrared frequency comb based on a quantum cascade laser," Nature 792(7428), 229-233 (2012).
[9] Villares, G. et al., "Dispersion engineering of quantum cascade laser frequency combs," Optica 3, 252 (2016).
[10] Villares, G., Hugi, A., Blaser, S. and Faist, J., "Dual-comb spectroscopy based on quantum-cascade-laser frequency combs," Nature Communications 5, 5192 (2014).

[11] Wang, Y., Soskind, M. G., Wang, W. and Wysocki, G., "High-resolution multi-heterodyne spectroscopy based on Fabry-Perot quantum cascade lasers," Applied Physics Letters 104, 31114 (2014).
[12] Hangauer, A., Westberg, J., Zhang, E. and Wysocki, G., "Wavelength modulated multiheterodyne spectroscopy using Fabry-Pérot quantum cascade lasers," Opt. Express, OE 24, 25298–25307 (2016).
[13] Sterczewski, L. A., Westberg, J. and Wysocki, G., "Molecular dispersion spectroscopy based on Fabry-Pérot quantum cascade lasers," Optics Letters. in press, (2017).
[14] Mansuripur, T. S., Vernet, C., Chevalier, P., Aoust, G., Schwarz, B., Xie, F. and Day, T., "Single-mode instability in standing-wave lasers: The quantum cascade laser as a self-pumped parametric oscillator," Physical Review A, 94(6), 063807 (2016).
[15] Herr, T. et al., "Universal formation dynamics and noise of Kerr-frequency combs in microresonators," Nat Photon 6, 480–487 (2012).
[16] Sterczewski L.A., Westberg J., and Wysocki G., "Tuning properties of mid-infrared Fabry-Pérot quantum cascade lasers for multiheterodyne spectroscopy," Photonics Lett Pol, vol. 8, no. 4, pp. 113–115, (2016).
[17] Schiller, S., "Spectrometry with frequency combs," Opt. Lett. 27, 766 (2002).
[18] Burghoff, D., Yang, Y. and Hu, Q., "Computational multiheterodyne spectroscopy," Science Advances, 2(11), p.e1601227 (2016).